Doubly differential multiple ionization of krypton by positron and electron impact

A. C. F. Santos, A. Hasan, and R. D. DuBois
University of Missouri-Rolla, Rolla, Missouri 65409, USA
(Received 20 November 2003; published 16 March 2004)

Measurements of doubly differential single and multiple ionization of krypton atoms have been performed for 750 eV positron and electron impact. Data were measured as a function of projectile energy-loss and scattering angle. For electrons, the energy-loss range was 0–85% of the initial projectile energy and scattering angles were between ±22°. Following the procedure adopted previously for argon, the electron impact data were placed on an absolute scale by normalizing to total ionization cross sections available in the literature. The present results for krypton show differences between positron and electron impact that are less pronounced than was found for argon. The difference between the two targets can be understood due to the role of inner-shell ionization.

DOI: 10.1103/PhysRevA.69.032706 PACS number(s): 34.80.Dp, 34.85.+x

I. INTRODUCTION

Total and differential single- and multiple-ionization cross sections of krypton by particles and antiparticles have been measured by many groups [1–12]. For positron impact, only two studies exist [7,8]. On the other hand, little differential information exists in the literature about multiple ionization of Kr atoms. One study by El-Sherbini and Van der Wiel [12] consists of small-angle inelastically scattered 10 keV electrons where oscillator strengths for multiple ionization of krypton were determined. In another study, Chaudhry *et al.* [13] measured partial doubly differential cross sections for multiple ionization of heavy noble gases by electron impact. The cross sections were measured as a function of ejected electron energy for electrons emitted 90° to the incident beam direction.

The present study adds to existing information and, in particular, makes a direct comparison between positron and electron impact data. In comparing single- and multiple-ionization cross sections resulting from electron and positron impact at high projectile velocities, simple first-order theories predict a q^2 dependence for the single-ionization cross sections. Here q is the projectile charge. In contrast, for double ionization at intermediate to lower velocities, interference effects between the so-called shake-off and two-step mechanisms can lead to differences associated with the projectile charge. Also, numerous conceptual argumentations such as change of the binding energies of the target electrons, change of the projectile trajectory, momentum transfer to the target, inner-shell contributions, or differences coming from postcollison interaction have been invoked to explain differences in total cross sections resulting from electron and positron impact [14,15].

In a previous work [16], doubly differential cross sections (DDCS) for single and multiple ionization of argon by electron impact were presented and compared to ionization yields for positron impact. The cross sections were measured as a function of projectile energy loss and scattering angle. Increasing differences were found between electron and positron impact cross sections as the degree of target ionization increased. In this paper, we extend these studies to the Kr target. This allows us to address the problem of the role played by larger target polarizability and inner-shell ionization.

Previously, only total cross section differences between positron and electron impact ionization have been studied as a function of target atomic number [8]. The present work provides more detailed information where charge related differences are studied as a function of energy loss and scattering angle. For example, the processes studied in this paper can be written as

$$e^{\pm}(E) + Kr \rightarrow e^{\pm}(E - \Delta E, \Delta\theta, \Delta\phi) + Kr^{n+} + ne^{-}. \qquad (1)$$

Here E is the initial projectile energy and ΔE is the energy loss, $\Delta\theta$ and $\Delta\phi$ are the azimuthal and polar scattering angular ranges sampled, and n is number of target electrons removed. For the present electron measurements, $\Delta\theta$ and $\Delta\phi$ are for forward scattering angles between ±22° and ±6.5°, respectively, and ΔE ranges from 0 up to 85% of the initial energy. For the present positron measurements, both $\Delta\theta$ and $\Delta\phi$ are for forward scattering angles less than ±22° and ΔE ranges from 0 to 25% of the initial energy.

II. EXPERIMENT

The experimental setup and procedures were described previously [16–18]. In brief, positron and electron beams are produced using a ^{22}Na source and a tungsten moderator, the slow positrons via energy loss within the moderator and the electrons primarily via secondary emission from the surface. The beams are guided to the collision chamber by means of electrostatic lenses and a 15° electrostatic deflection. The deflection prevents unmoderated positrons and gammas from entering the scattering chamber. Switching from positron to electron beams is simply done by reversing all the bias and focusing/steering voltages, plus the postcollision beam energy analyzer voltages.

The beams intersect a jet of krypton gas emerging from a needle source. The forward-scattered projectiles are energy and angle analyzed by an electrostatic spectrometer and recorded by a microchannel plate position sensitive detector, located at the focal plane of the analyzer. The horizontal location on the detector is dependent of the final energy, E

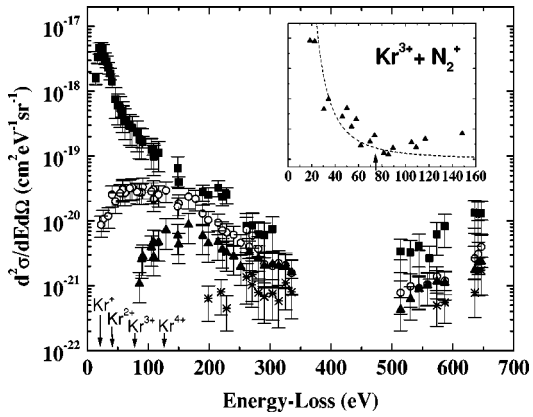

FIG. 1. Single (squares), double (circles), triple (triangles), and quadruple (stars) doubly differential electron impact cross sections for 750 eV electrons on Kr as a function of projectile electron loss for electrons scattered in the forward direction between $\varphi = 0 \pm 6.5°$ and $\theta = 0 \pm 22°$. Vertical arrows indicate the respective thresholds. The inset shows the raw $Kr^{3+} + N_2^+$ data as a function of the projectile energy loss and the threshold energy for triple ionization of krypton. The dotted line represents a fit of (ax^b) below threshold. Above the Kr^{3+} ionization threshold, the fitted function was extrapolated in order to subtract the N_2^+ contribution.

$-\Delta E$, and the vertical location on the scattering angle $\Delta\theta$. For the present electron impact studies, the horizontal and vertical acceptance angles are ±6.5° and ±22°, respectively, and the angular resolution is 2°. The energy resolution of the secondary electron emission source is roughly 12 eV (full width at half maximum), while the corresponding energy spread for the positron beam is less than 2 eV.

The ionized recoil ions are extracted from the collision region by a weak electric field (10 V/cm), separated according to their mass-to-charge ratio by a time-of-flight spectrometer and detected by another microchannel plate detector. The recoil ions are used as the stop signal to a time-to-digital converter which is started by the signals from the projectile detector. By setting windows on the time-of-flight spectra, differential energy-loss spectra could be measured for multiple as well as for single ionization. The total number of recoil ions are used to normalize data recorded for different energy-loss ranges and to place all data on an absolute scale. Singly and doubly charged recoil ions could be clearly distinguished from random background coincidences, but the Kr^{3+} peak could not be separated in flight time from N_2^+. However, in the following section we present a procedure to subtract the contribution of the N_2^+.

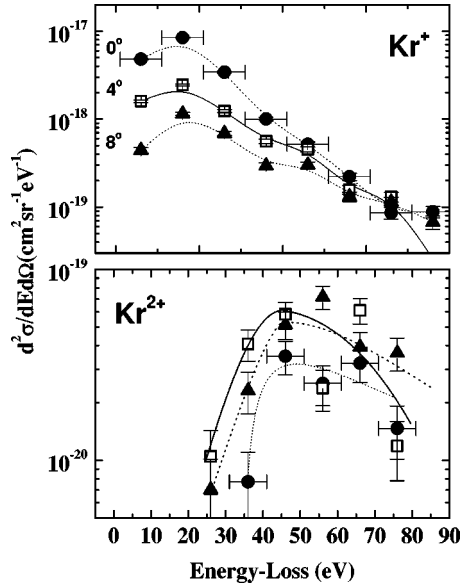

FIG. 2. Doubly differential cross sections for single (top figure) and double (bottom figure) ionization of Kr by 750 eV electron impact as a function of the projectile electron loss. Data are for $\varphi = 0 \pm 6.5°$ and selected scattering angles $\theta = 0°$ (circles), 4° (squares), and 8° (triangles). Curves serve only to guide the eye.

III. RESULTS

Differential information for single, double, triple, and quadruple ionization of the Kr *N* and *M* shells are presented in Figs. 1–4. Following the procedure presented in a previous work, the electron impact data were put on an absolute scale by normalization to the total cross-sectional data of Sorokin *et al.* [5]. To convert the measured coincidence signals to absolute cross sections we use the fact that the DDCS are given by

$$\frac{d^2\sigma^{q+}}{d\Omega dE} = \frac{N_R^{q+}(\Omega, E - \Delta E)}{\varepsilon^{q+}(N_P/\varepsilon_P) N_T \Delta\Omega \Delta E'}. \tag{2}$$

Here $N_R^{q+}(\Omega, E - \Delta E)$ is the number of recoil ions of charge state q measured in coincidence with projectiles having a

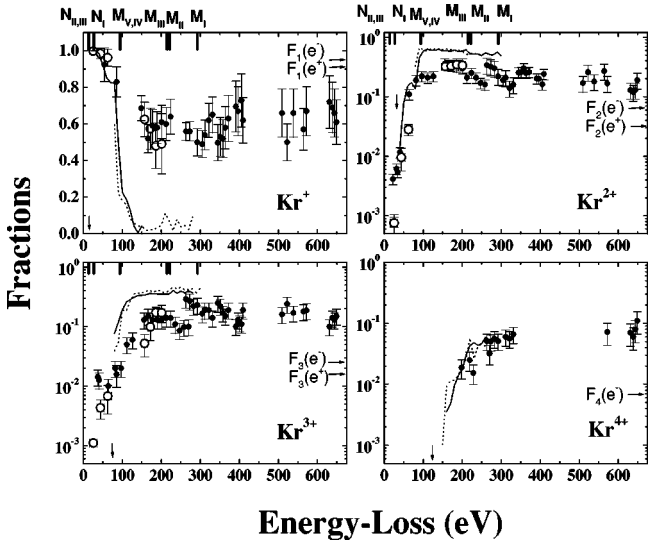

FIG. 3. Fractions of single, double, triple, and quadruple ionization by positron (open circles), electron (closed circles and solid curves), and photon (dotted curves) impact. Data are for projectiles scattered in the forward direction as a function of the projectile energy loss. For electron impact, $\varphi = 0 \pm 6.5°$ and $\theta = 0 \pm 22°$; for positron impact, φ and $\theta = 0 \pm 22°$. Vertical lines indicate the binding energies of *N* and *M* shells. Vertical arrows indicate the threshold energies for single, double, etc., ionization, while horizontal arrows indicate the fractions determined using total cross sections from Refs. [21,22]. The solid curves are for high-energy electron impact [12] while the dotted curves are photoionization data [25].

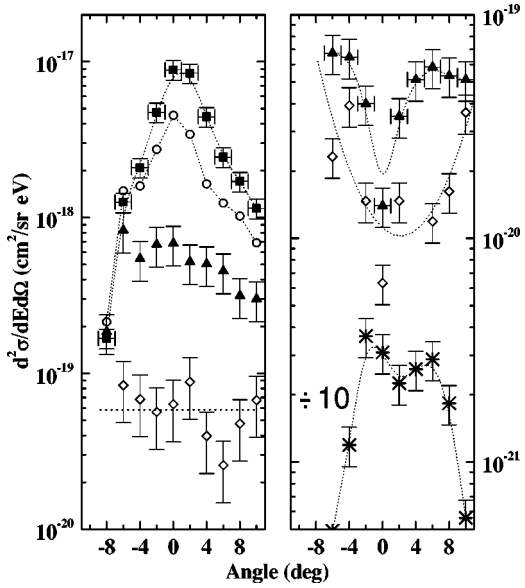

FIG. 4. Single and double doubly differential cross sections for 750 eV electrons on Kr as a function of the scattering angle for selected projectile energy losses. Left figure, single ionization; right figure, double ionization. Squares, $\Delta E=16$ eV; circles, $\Delta E=26$ eV, triangles, $\Delta E=46$ eV; diamonds, $\Delta E=76$ eV; stars, $\Delta E=96$ eV, divided by 10 for display purposes. The curves are to guide the eye.

final energy $E-\Delta E$ that are scattered into a solid angle Ω. N_T is the number of target atoms, N_p is the beam intensity (number of projectiles), ε^{q+} and ε_p are the recoil ion and scattered projectile detection efficiencies, $\Delta\Omega$ and $\Delta E'$ are the projectile solid angle and the energy range accepted, respectively.

We do not measure N_p or N_T directly. Instead, we measure the number of recoils which are related to the former quantities and the gross ionization cross section σ as follows:

$$\sum_q q\frac{N_R^{q+}}{\varepsilon^{q+}} = N_P N_T \sigma. \tag{3}$$

The left side can be rewritten as

$$\sum_q q\frac{N_R^{q+}}{\varepsilon^{q+}} = N_R \sum_q q\frac{F^{q+}}{\varepsilon^{q+}}, \tag{4}$$

where F^{q+} are the fractions of single, double, triple, etc. ionization and N_R are the total number of recoils. The fractions were measured quantities taken from Fig. 3 and the recoil ion detection efficiencies were taken from Ref. [19]. Finally, in Eq. (2) the scattered projectile detection efficiencies which include transmission through one grid in our setup, were taken from Müller *et al.* [20].

The positron impact data were obtained prior to making this calibration. Hence, for positron impact only fractions of single and multiple ionization are presented.

A. Energy-loss dependence

Using these procedures, absolute single, double, triple, and quadruple ionization of Kr by 750 eV electron impact were determined and are shown in Fig. 1 as a function of the projectile energy loss. The data are for all electrons scattered in a forward direction for angles θ and ϕ between ±22° and ±6.5°. Even though one cannot distinguish whether the detected electron is a scattered primary or ionized target electron, kinematic arguements imply that the first half, $E<375$ eV, should consist primarily of scattered projectile electrons, while the second half, $E>375$ eV, has ever increasing contributions from ejected target electrons.

To subtract the contribution of the N_2^+ ion from the triple ionization of krypton the following procedure was used. The ionization potentials for producing N_2^+ and Kr^{3+} ions are 15.51 and 75.3 eV. Our krypton single-ionization data show a sharp decrease in the ionization cross section for energy losses above the ionization threshold. The inset in Fig. 1 shows the raw $Kr^{3+}+N_2^+$ data where a similar sharp decrease is seen between 20 and 80 eV followed by a slow increase for larger energy losses. We attribute the decrease to the N_2^+ contribution and the increase to the onset of triple ionization of krypton. Therefore we fit the data below 75.3 eV with a decreasing background (allometric function) in order to extrapolate and subtract the N_2^+ contribution above 75 eV. The fit is shown in the inset with the residual Kr^{3+} cross section shown in the main figure.

The experimental data demonstrate that single ionization of krypton has a narrow maximum at about 25 eV, decreases quite rapidly for the first 50 eV of energy loss then more slowly throughout the first half of the available energy-loss range. Above 500 eV the increase is attributed to ejected target electrons. The double ionization presents a broad maximum around 80 eV. Above 100 eV, the double ionization has roughly the same energy dependence as single ionization. Triple ionization has a broad maximum around 150 eV. Around 300 eV, triple ionization cross sections are roughly as large as double ionization. Quadruple ionization is not observed in the present experiment until ~200 eV which is well after the $M_{V,IV}$ shell opens (~100 eV).

Figure 2 shows the DDCS for single, double, and triple ionization of Kr as a function of energy loss for selected projectile scattering angles. For small energy losses, single ionization dominates but decreases rapidly with increasing scattering angle. For larger energy losses and the small range of scattering angles investigated here, single ionization is fairly isotropic. The lower half of Fig. 2 shows a much different behavior for double ionization. For the first 50 eV above the double ionization threshold, the double ionization intensity increases between 0° and 4° and then decreases slightly between 4° and 8°. Figure 2 also shows that for scattering angles between 0° and 8°, as the projectile energy loss increases the relative amount of double to single ionization increases.

B. Comparison between electron, positron, and photon impact

The fractions of single and multiple ionization of Kr by positron and electron impact as a function of energy loss are plotted in Fig. 3. The data are for positrons scattered between θ,φ between ±22° and electrons between $\theta=\pm 22°$ and $\varphi=\pm 6.5°$. As seen in Figs. 2 and 4 using different ranges in φ does not influence this comparison since angles between 6.5°

and 22° do not significantly contribute to the cross sections. Single target ionization dominates over the entire range of energy loss. Its contribution decreases from 100% near the threshold down to 60% at 200 eV, just below the $M_{III,II}$ shell edge, then remains constant. For large energy losses, where the coincidence rate was very low, there is scatter in the measured values but the overall trend is obvious. The percentage of double ionization increases rapidly for the first 100 eV, reaches a maximum of 35% around 200 eV and then falls slowly to 20% at 650 eV. Triple ionization also shows a fast increase, reaching a maximum of roughly 15% after the $M_{III,II}$ shell is opened after which it remains constant. For electron impact, quadruple ionization reaches its maximum of roughly 8% at 300 eV and also remains constant.

Figure 3 also compares the positron and electron data. At lower-energy losses, the fractions of single ionization by positron impact are larger than the corresponding factions for electron impact. Above 150 eV, both fractions are roughly the same. The relative amount of double ionization is systematically higher for electron than for positron impact until 200 eV, where both fractions merge. Unfortunately, due to the low statistics, no data for positron impact after the $M_{III.II}$ shell ionization threshold were obtained. A projectile charge effect is also observed in the triple ionization of krypton. Here again, both curves seem to merge around 200 eV. These charge effects were also observed in the total multiple-ionization cross sections where the electron impact data are larger than the positron impact data [21,22]. The corresponding fractions for total single, double, triple, and quadruple ionization by electron (positron) impact are 0.90(0.95), 0.064(0.033), 0.026(0.017), and 0.071(–), indicated by the horizontal arrows in Fig. 3. To the knowledge of the authors, there are no previous measurements of quadruple ionization of krypton by positron impact.

Projectile charge effects have been attributed to interference between the shake-off and two-step mechanisms [23]. At large impact parameters, corresponding to small momentum transfer and consequently to small energy losses, the shake-off mechanism is expected to dominate over the two-step mechanism, which peaks at smaller impact parameters b. Using the adiabaticity criterion [24]

$$b = \frac{\hbar v}{\Delta E}, \tag{5}$$

where ΔE is the inelastic energy transfer and ν is the projectile velocity, one can estimate the impact parameter for the most significant contribution to the cross section at a given projectile energy loss. In the present experiment the smallest possible impact parameter corresponding to total-energy loss by the projectile is ~0.3 a.u., while for ΔE given by the various ionization potentials, the maximum impact parameter is roughly 14, 5, 3, and 1.6 a.u. for single, double, triple, and quadruple ionization, respectively.

Another explanation for the observed charge effects is the Coulomb effect, which means that positively and negatively charged projectiles will follow different trajectories as they pass through the target field [22]. Since ionization probabilities are larger for close compared to distant collisions, the positron multiple-ionization cross sections are reduced due to the Coulomb effect which prevents positrons from penetrating deep into the target atom. On the other hand, electrons are attracted to the target nucleus, sinking in deeper compared to positrons, so that the ionization takes place at reduced impact parameters closer to the maximum of the ionization probability.

However, our data indicate that differences between multiple ionization by positron and electron impact are less pronounced in krypton than for argon. For instance, in the case of triple ionization of Ar, the electron impact fractions were found to be three times the positron impact ones at large projectile energy losses. For krypton, no significant differences between the positron and electron impact fractions at large projectile energy losses are seen. This is most likely due to the increasing influence of inner-shell processes for the heavier target krypton.

Figure 3 also compares the electron and positron impact data with photoionization data from Refs. [25,12]. The fractions of single ionization by positron, electron and photon impact agree with each other below 100 eV, i.e., before the $M_{V,IV}$ shell is opened. The fractions of double ionization by photon impact are systematically above their corresponding for positron and electron impact. The same holds for the triple ionization. On the contrary, the fractions of quadruple ionization by photon impact are in a quite good agreement with the electron impact data.

C. Angular distributions

In Fig. 4 the scattering angle dependence of projectile electrons is shown for several energy losses. The left side shows dependences for single electron removal while the right side shows data for double ionization. For single ionization, the DDCS have maxima at 0°. As the projectile energy loss increases, the angular distributions become broader with the intensity at 0° decreasing rapidly until the distributions become isotropic. These characteristics are well known and come from ever decreasing impact parameters which lead to larger and larger momentum transfer to the target electron.

For double ionization the distributions are entirely different. For lower-energy losses, the cross sections have a minimum for projectile scattering angles near 0°. For energy losses only slightly larger than the double ionization threshold, the cross section maximizes around 6°. For a 76 eV energy loss no maximum is observed. Presumably, the maximum occurs outside the range of scattering angles investigated. At a 96 eV energy loss the double ionization cross section presents a different behavior. A shallow minimum can still be seen around 0°, but this is followed by a maximum around 4° and a fast decrease for larger scattering angles. We do not understand this behavior but point out that it should not be associated with low statistics as the cross section for a 100 eV energy loss leading to double ionization is still quite large (see Fig. 1).

These double ionization angular behaviors may be explained in a couple of ways. Using kinematic arguments, double ionization takes place at small impact parameters which means that it is more likely that the projectile deflects

rather than traveling straight ahead. For example, Kamber *et al.* [26] observed a maximum around 4° for 46 eV projectile energy loss leading to double ionization of Ne and Ar in collisions with fast protons. Giese and Horsdal [27] measured the fractions of doubly charged He ions generated by 300–1000 keV protons on He and also observed a maximum. These structures in the differential cross section were discussed by Végh [28] who suggested that the peak could be explained by the kinematics of a multiple-scattering mechanism. Following a violent projectile-electron collision, the scattered electron knocks out a second electron and a second projectile-electron collision takes place.

IV. SUMMARY AND CONCLUSIONS

We have presented absolute and partial differential information for single and multiple ionization of krypton for 750 eV positron and electron impact. These data demonstrate that the relative amount of multiple ionization increases with energy loss for both projectiles. The data demonstrate that single and multiple ionization in the outermost *N* shell of krypton atom dominate. At higher-energy losses, single ionization dominates with a branching ratio of ~60%, followed by double and triple ionization with branching ratios roughly 20% and 15%. The differences in the multiple ionization by positron and electron impact are smaller than those observed previously for ionization of argon and have been discussed in terms of the interference and Coulomb effects.

ACKNOWLEDGMENTS

This work was supported by National Science Foundation (Grant No. PHY0097902). A.C.F.S. is grateful for support from CNPq (Brazil) and the hospitality received during his staying at UMR.

[1] S. Denifl, B. Gstir, G. Hanel, L. Feketeova, S. Matejcik, K. Becker, A. Stamatovic, P. Scheier, and T. D. Mark, J. Phys. B **35**, 4685 (2002).
[2] D. P. Almeida, Int. J. Mass. Spectrom. **184**, 49 (1999).
[3] P. Nagy, A. Skutlartz, and V. Schmidt, J. Phys. B **13**, 1249 (1980).
[4] R. Rejoub, B. G. Lindsay, and R. F. Stebbings, Phys. Rev. A **65**, 042713 (2002).
[5] A. A. Sorokin, L. A. Shmaenok, S. V. Bobashev, B. Mobus, H. Richter, and G. Ulm, Phys. Rev. A **61**, 022723 (2000).
[6] A. Kobayashi, G. Fujiki, A. Okaji, and T. Masuoka, J. Phys. B **35**, 2087 (2002).
[7] S. Helms, U. Brinkmann, J. Dewikis, R. Hippler, H. Schneider, D. Segers, and J. Paridaens, J. Phys. B **28**, 1095 (1988).
[8] V. Kara, K. Paludan, J. Moxon, P. Ashley, and G. Laricchia, J. Phys. B **30**, 3933 (1997).
[9] W. S. Melo, A. C. F. Santos, M. M. Sant'Anna, G. M. Sigaud, and E. C. Montenegro, J. Phys. B **35**, L187 (2002).
[10] R. D. DuBois, Phys. Rev. A **33**, 1595 (1986).
[11] R. D. DuBois, l. H. Toburen, and M. E. Rudd, Phys. Rev. A **29**, 70 (1984).
[12] Th. M. El-Sherbini and M. J. Van der Wiel, Physica (Amsterdam) **62**, 119 (1972).
[13] M. A. Chaudhry, A. J. Duncan, R. Hippler, and H. Kleinpoppen, Phys. Rev. A **39**, 530 (1989).
[14] D. R. Schultz, R. E. Olson, and C. O. Reinhold, J. Phys. B **24**, 521 (1991).
[15] H. Knudsen and J. F. Reading, Phys. Rep. **212**, 107 (1992).
[16] A. C. F. Santos, A. Hasan, T. Yates, and R. D. DuBois, Phys. Rev. A **67**, 052708 (2003).
[17] R. D. DuBois, C. Doudna, C. Lloyd, M. Kahveci, Kh. Khayyat, Y. Zhou, and D. H. Madison, J. Phys. B **34**, L783 (2001).
[18] R. D. DuBois, Kh. Khayyat, C. Doudna, C. Lloyd, Nucl. Instrum. Methods Phys. Res. B, **192**, 63 (2002).
[19] R. D. DuBois, Phys. Rev. A **36**, 2585 (1987).
[20] A. Müller, N. Djurić, G. H. Dunn, and D. S. Belić, Rev. Sci. Instrum. **57**, 349 (1986).
[21] R. Rejoub, B. G. Lindsay, and R. F. Stebbings, Phys. Rev. A **65**, 042713 (2002).
[22] S. Helms, J. Phys. B **28**, 1095 (1995).
[23] J. H. McGuire, Phys. Rev. Lett. **49**, 1153 (1982).
[24] H. Knudsen, L. H. Andersen, H. K. Haugen, and P. Hvelplund, Phys. Scr., T **26**, 132 (1982).
[25] D. M. P. Holland, K. Codling, J. B. West, and G. V. Marr, J. Phys. B **12**, 2465 (1979).
[26] E. Y. Kamber, C. L. Cocke, S. Cheng, and S. L. Varghese, Phys. Rev. A **41**, 150 (1990).
[27] J. P. Giese and E. Horsdal, Phys. Rev. Lett. **60**, 2018 (1988).
[28] L. Végh, J. Phys. B **22**, L35 (1989).